Cardiovascular Research (2011) **91**, 310–319
doi:10.1093/cvr/cvr081

Regulation of murine cardiac contractility by activation of α_{1A}-adrenergic receptor-operated Ca^{2+} entry

Marion C. Mohl[1], Siiri E. Iismaa[1,2], Xiao-Hui Xiao[1], Oliver Friedrich[3], Soeren Wagner[3], Vesna Nikolova-Krstevski[1], Jianxin Wu[1], Ze-Yan Yu[1], Michael Feneley[1,2,4], Diane Fatkin[1,2,4], David G. Allen[5], and Robert M. Graham[1,2,4]*

[1]Molecular Cardiology and Biophysics Division, Victor Chang Cardiac Research Institute, Lowy Packer Building, 405 Liverpool St, Darlinghurst, NSW 2010, Australia; [2]University of New South Wales, Kensington, NSW 2052, Australia; [3]Medical Biotechnology, Friedrich-Alexander-University, 91052 Erlangen, Germany; [4]St.Vincent's Hospital, Darlinghurst, NSW 2010, Australia; and [5]Physiology Department, University of Sydney, Sydney, NSW 2006, Australia

Received 30 January 2011; revised 3 March 2011; accepted 16 March 2011; online publish-ahead-of-print 5 May 2011

Time for primary review: 18 days

Aims Sympathetic regulation of cardiac contractility is mediated in part by α_1-adrenergic receptors (ARs), and the α_{1A}-subtype has been implicated in the pathogenesis of cardiac hypertrophy. However, little is known about α_{1A}-AR signalling pathways in ventricular myocardium. The aim of this study was to determine the signalling pathway that mediates α_{1A}-AR-coupled cardiac contractility.

Methods and results Using a transgenic model of enhanced cardiac α_{1A}-AR expression and signalling (α_{1A}-H mice), we identified a receptor-coupled signalling pathway that enhances Ca^{2+} entry and increases contractility. This pathway involves α_{1A}-AR-activated translocation of Snapin and the transient receptor potential canonical 6 (TRPC6) channel to the plasma membrane. In ventricular cardiomyocytes from α_{1A}-H and their non-transgenic littermates (or WTs), stimulation with α_{1A}-AR-specific agonists resulted in increased $[Ca^{2+}]_i$, which was dose-related and proportional to the level of α_{1A}-AR expression. Blockade of TRPC6 inhibited the α_{1A}-AR-mediated increase in $[Ca^{2+}]_i$ and contractility. External Ca^{2+} entry, underlying the $[Ca^{2+}]_i$ increase, was not due to store-operated Ca^{2+} entry but to a receptor-operated mechanism of Ca^{2+} entry resulting from α_{1A}-AR activation.

Conclusion These findings indicate that Ca^{2+} entry via the α_{1A}-AR-Snapin-TRPC6-pathway plays an important role in physiological regulation of cardiac contractility and may be an important target for augmenting cardiac performance.

Keywords α_{1A}-AR • TRPC • Cardiac contractile function • Cell signalling • Calcium cycling

1. Introduction

Adrenergic receptor (AR) activation in response to sympathetic nervous system stimulation has a major role in regulating cardiac function.[1,2] Cardiomyocytes (CMs) express both α- and $\beta_{1/2}$-ARs. In normal adult hearts, cardiac inotropy and chronotropy are predominantly regulated by β_1-ARs.[1] Under pathological conditions, however, e.g. myocardial ischaemia or hypertrophy, α_1-ARs function in a compensatory fashion to maintain cardiac inotropy when β_1-ARs are down-regulated[1,3] and uncoupled from G proteins and effectors.[4] In addition, although implicated in the pathogenesis of hypertrophy,[5] α_1-ARs, particularly the α_{1A}-subtype, are important in both developmental CM growth and survival.[5,6]

Cardiac α_1-AR stimulation enhances contractility and causes small but significant increases in $[Ca^{2+}]_i$, but underlying mechanisms remain incompletely understood. It has been suggested that α_1-AR -activation is associated with coupling to the $G_{q/11}$ family of heterotrimeric G proteins and phospholipase Cβ (PLCβ) isoform-activation,[7] resulting in phosphatidylinositol(4,5)-*bis*phosphate hydrolysis to inositol(1,4,5)-trisphosphate (IP_3) and diacylglycerol (DAG). This results in Ca^{2+} mobilization from intracellular stores and Ca^{2+} membrane influx.[8] Elevated $[Ca^{2+}]_i$ might also be due to (i) store-operated

* Corresponding author. Tel: +61 2 9295 8602; fax: +61 2 9295 8601, Email: b.graham@victorchang.edu.au

channels (SOCs) activated, for example, by IP_3-induced Ca^{2+} depletion of internal stores or (ii) via receptor-operated channels (ROCs).[9] It is unclear whether these pathways are major contributors to CM α_1-AR signalling, since PLCβ activity and IP_3 generation as well as IP_3-receptor (IP_3R) expression are generally low in CMs.[10]

Transient receptor potential (TRP) proteins form non-selective cationic channels that are implicated in diverse biological functions,[11] and changes in the expression of canonical TRP channels (TRPCs) have been linked to cardiac hypertrophy development.[11,12] Some studies suggest that TRPCs act as SOCs; others have shown that they can also function as ROCs.[13] In PC12 cells, interactions between TRPC6 and the adaptor protein, Snapin, regulate α_{1A}-AR-mediated Ca^{2+} influx[14]—Snapin being a SNARE-associated modulatory protein involved in exocytosis and cytokinesis.[15,16]

Here, we utilized a transgenic mouse model with cardiac-restricted α_{1A}-AR overexpression to show that TRPC6–Snapin interactions determine α_{1A}-AR signalling, both in isolated CMs and *in vivo*. In this transgenic model, mice with four-fold α_{1A}-AR overexpression (α_{1A}-L) are phenotypically normal, while mice with 66-fold (α_{1A}-M) and 170-fold (α_{1A}-H) overexpression display expression-related increases in systolic contractile function.[17] Interestingly, despite increased α_{1A}-AR expression, none of these mice showed cardiac hypertrophy under baseline conditions, and hypertrophic responses to pressure overload were similar to those in wild-type (WT) littermates.[18] Moreover, while enhanced α_{1A}-AR-drive in the α_{1A}-M line improved survival in response to myocardial infarction or pressure overload,[18,19] the α_{1A}-H line is susceptible to sudden cardiac death characterized by a rapid reduction in QRS amplitude in the absence of significant brady- or tachyarrhythmias.[20] Here, we show that stimulation of α_{1A}-ARs results in a dynamic interaction of Snapin and TRPC6 resulting in receptor-operated Ca^{2+} entry (ROCE), and that blockade of this pathway prevents sudden cardiac death in α_{1A}-H mice. Although an increase in $[Ca^{2+}]_i$ upon α_{1A}-AR activation is barely detectable in normal CMs, this α_{1A}-AR-coupled Ca^{2+} entry pathway is associated with augmented contractility even in WT hearts. Furthermore, enhancement of this signalling pathway underlies both the hypercontractility of α_{1A}-H mice and the sudden death observed in this transgenic model.

2. Methods

2.1 Animals

Transgenic male mice with cardiac-specific overexpression[17] (α_{1A}-H, 170-fold; α_{1A}-M, 66-fold) of the rat α_{1A}-AR on a FVB/N genetic background, and their non-transgenic littermates (or WTs), were studied at 2–4 months of age. All experimental procedures were approved by the Garvan/St Vincent's Hospital Animal Ethics Committee, in accordance with the guidelines of the Australian Code of Practice for the Care and Use of Animals for Scientific Purposes. The investigation conforms with the Guide for the US National Institutes of Health's Care and Use of Laboratory Animals (NIH Publication no 85–23, revised 1996).

2.2 Development of pore inhibitory anti-TRPC1 and TRPC6 antibodies

Rabbit anti-TRPC1 and anti-TRPC6 antibodies, raised (Peptide Specialty Laboratories GmbH, Heidelberg, Germany) against the putative pore-forming loop of these TRPCs, were immunoaffinity-purified using the respective peptide immunogens coupled to Cn-Br-activated agarose (see Supplementary material online, *Methods* for details).

2.3 Production of shRNA-encoding adenoviruses

Oligonucleotide sequences for shRNA1-Snapin, shRNA2-Snapin, or shRNA scrambled (see Supplementary material online, *Methods*) were cloned into the multiple cloning site of pAdTrack-si,[21] and recombinant adenoviruses were generated as described.[22]

2.4 Reverse transcriptase–polymerase chain reaction

Snapin, TRPC1, TRPC6, and porphobilinogen deaminase cDNAs were generated from mouse total RNA as detailed in Supplementary material online, *Methods*.

2.5 Immunoblot analysis

Western blotting was performed using antibodies to Snapin, TRPC1, or TRPC6 (see Supplementary material online, *Methods*).

2.6 Cell lines, culture, and transfection

HEK293 and COS cells were cultured in high-glucose Dulbecco's modified Eagle's medium (see Supplementary material online, *Methods*) and transfected using Lipofectamine 2000 (Invitrogen).

2.7 Isolation, cell culture, and adenoviral infection of ventricular adult mouse CMs

α_{1A}-H and α_{1A}-M and WT mice were anesthetized with Nembutal (60 mg/kg, ip; anaesthesia depth was monitored by limb withdrawal using toe pinching), a thoracotomy was performed and left ventricular CMs isolated from the hearts by enzymatic retrograde perfusion,[23] as detailed in Supplementary material online, *Methods*, were incubated for 1 h at 37°C and 2% CO_2 in plating media (MEM media containing 10% FCS, 10 mM BDM, 2 mM Penicillin/Streptomycin, 2 mM Glutamine). CMs were then washed two times with culturing media (MEM media containing 0.5% FCS, 2 mM penicillin/streptomycin, 2 mM glutamine) and cultured in culturing media at 37°C and 2% CO_2, with or without adenovirus at MOI 100, for 96 h.[24]

2.8 Immunocytochemistry

CMs cultured on laminin-coated glass coverslips were stimulated with methoxamine (100 μmol/L), A61603 (100 nmol/L) and/or prazosin (100 nmol/L), fixed, permeabilized and stained for Snapin, TRPC1, or TRPC6, as detailed in Supplementary material online, *Methods*.

2.9 Transmission electron microscopy and immunogold labelling

Cardiac tissue sections were stained with TRPC1 or TRPC6 with 10 nm colloidal-gold-conjugated antibody, and for Snapin or caveolin antibodies with 20 nm colloidal-gold-conjugated antibody, as detailed in Supplementary material online, *Methods*. Pictures were taken at ×50 000 magnification.

2.10 Measurement of $[Ca^{2+}]_i$

Ca^{2+} recordings were performed either using batches of isolated, fura-2 AM-loaded CMs in a cuvette to quantify mean fluorescence, or using single-isolated fluo-4 AM-loaded CMs monitored by confocal Ca^{2+} microscopy (for details, see Supplementary material online, *Methods*).

2.11 Isolated heart perfusions

Animals were anaesthetized (Nembutal, 60 mg/kg, ip) and a thoracotomy was performed, and hearts from α_{1A}-H or WT mice were isolated for Langendorff perfusion (detailed in Supplementary material online, *Methods*). Seven to eight animals were analysed per group.

2.12 Co-immunoprecipitation

Animals were anesthetized (1.5% isofluorane in medical grade O_2 delivered by nose cone; anaesthesia depth was monitored by limb withdrawal using toe pinching) and a 1.4 Fr Millar catheter introduced in the left carotid artery to monitor arterial blood pressure. After measurement of baseline parameters, saline or PE (WT 100 μg/kg; α_{1A}-AR-H 3.3 μg/kg in 25 μL) was delivered over 1 min into the left jugular vein with a 100 μL Hamilton syringe using an sp200i syringe pump. Prazosin (0.5 mg/kg, in 25 μL, ip, 1 min incubation) was administered as a bolus in a volume of 1 mL/kg as indicated. Hearts were quickly extracted at the times indicated, membrane fractions were prepared, solubilized, precleared, incubated with Snapin-FL-antibody covalently coupled to G-sepharose, and proteins eluted for SDS–PAGE electrophoresis as described in Supplementary material online, *Methods*.

2.13 Data analysis

Results shown are means ± 1SD. Statistical differences were determined by two-way analysis of variance (two-way ANOVA) for quantification of intensity staining and Ca^{2+} recordings and one-way ANOVA for isolated hearts followed by a pairwise comparison, with $P \leq 0.05$ being considered significant.

3. Results

3.1 Endogenous expression and subcellular localization of TRPC6, TRPC1, and Snapin in CMs and heart tissue

Immunoblot (*Figure 1A*, left panel) and densitometric analyses (data not shown) revealed Snapin, TRPC6, and TRPC1 expression in isolated CMs and in myocardium of α_{1A}-H and WT mice. Snapin and TRPC6 expression levels were more marked in the myocardium, suggesting that their expression is not limited to CMs, but also occurs in non-CMs. In contrast, expression of TRPC1, a well-characterized SOC, was similar in myocardium and in CMs, indicating predominant CM expression. Transmission electron microscopy (TEM) of immunogold-labelled α_{1A}-H and WT myocardium showed co-localization of Snapin, TRPC6, and TRPC1 in the plasma membrane and the t-tubules; the latter evident from caveolin-3 immunolabelling (*Figure 1B*). Specificity of antibody staining was confirmed by blockade of immunoblotting (*Figure 1A*, right panel) with the peptide immunogens used to generate anti-TRPC6 and anti-TRPC1 antibodies.

3.2 Dynamic interaction of α_{1A}-AR, Snapin, and TRPC6 *in vitro* and *in vivo*

Prior to CM stimulation with a commonly used α_1-AR agonist, methoxamine, TRPC6, and Snapin were evident in both the plasma membrane and t-tubules as well as in the cytosol of WT CMs (*Figure 2A–C*), with slightly higher plasma membrane vs. intracellular localization in unstimulated α_{1A}-H CMs (*Figure 2B* and *C*). α_1-AR activation resulted in translocation of Snapin and TRPC6 from the t-tubules to the plasma membrane in both WT and α_{1A}-H CMs, as evident by the loss of tubular staining and a weaker striation pattern (*Figure 2A*). This translocation was abrogated by pre-treatment with the α_1-AR-specific antagonist, prazosin. In WT CMs, recruitment to the plasma membrane peaked at 5–10 min after α_1-AR activation (*Figure 2B*), whereas in α_{1A}-H CMs, plasma membrane recruitment was faster (peaking at 2 min) (*Figure 2C*). In contrast to TRPC6, no significant plasma membrane translocation of TRPC1 was observed with α_1-AR activation of WT or α_{1A}-H CMs (see Supplementary material online, *Figure S1*).

Next, we investigated whether the interaction of α_{1A}-AR, Snapin, and TRPC6 observed *in vitro* was also operative *in vivo*. Hearts were rapidly excised from α_{1A}-H and WT mice after administration of phenylephrine (PE) to activate α_1-ARs or saline. Immunoprecipitation of solubilized membranes with an anti-Snapin antibody showed that α_{1A}-AR and TRPC6 (but not TRPC1; data not shown) co-immunoprecipitated with Snapin in both α_{1A}-H mice and WT hearts, even basally after saline administration, although this interaction was greater in α_{1A}-H mice (see Supplementary material online, *Figure S2*). In the WT, co-immunoprecipitation was maximal at 1.5 min and waned by 7 min after PE administration (see Supplementary material online, *Figure S2*). In both genotypes, this interaction was increased after α_1-AR activation, although to a greater extent in α_{1A}-H mice (see Supplementary material online, *Figure S2B*). These data indicate a dynamic interaction between α_{1A}-AR, Snapin, and TRPC6 *in vivo*.

3.3 Increased $[Ca^{2+}]_i$ in α_{1A}-M and α_{1A}-H relative to WT CMs after α_1A-AR activation

To provide more robust evidence for an interaction between α_{1A}-AR, Snapin, and TRPC6, we used the highly selective α_{1A}-AR agonist, A61603, in subsequent studies. Consistent with very low α_{1A}-AR expression in WT CMs,[1] receptor stimulation with A61603 resulted in only a slight increase in $[Ca^{2+}]_i$ in these cells, which was only significant at the highest A61603 dose (30 nM; *Figure 3A*). In contrast, dose-dependent tonic increases in $[Ca^{2+}]_i$, directly related to the level of α_{1A}-AR overexpression, were evident in α_{1A}-M and α_{1A}-H CMs, and were already highly significant with 1 nM A61603. At the highest (30 nM) A61603 dose, increases in $[Ca^{2+}]_i$ of up to ~1–1.5 μM were observed (*Figure 3A*). Similar increases in $[Ca^{2+}]_i$ have also been observed with field stimulation of CMs.[25] To confirm the specificity of the A61603-mediated increase in $[Ca^{2+}]_i$, we demonstrated that it could be abolished by pre-treatment with the α_{1A}-AR-selective antagonist, KMD3213 (*Figure 3B*).

3.4 Increase in $[Ca^{2+}]_i$ is triggered by ROCE upon α_{1A}-AR activation and requires TRPC6 and Snapin

To investigate whether α_{1A}-AR-stimulated tonic increases in $[Ca^{2+}]_i$ are due to Ca^{2+} influx through SOCs or ROCs,[26] we evaluated $[Ca^{2+}]_i$ both in batches of isolated CMs to carefully quantify the $[Ca^{2+}]_i$ signal, as well as in single-isolated cells. As shown in *Figure 3C*, addition of non-specific TRPC channel- and ROC/SOC inhibitors, La^{3+} or gentamicin, to batches of CMs from α_{1A}-H or WT mice suppressed α_{1A}-AR-mediated increases in $[Ca^{2+}]_i$, whereas inhibition of store-operated Ca^{2+} entry (SOCE) with 2-APB, or IP_3-mediated signalling with xestospongin C, had no effect. To demonstrate ROCE, CMs were treated with ROC/SOC inhibitors, La^{3+}, and gentamicin, as well as the SOCE inhibitor, 2-APB, after initial depletion of the sarcoplasmic reticulum (SR) Ca^{2+}-ATPase using cyclopiazonic acid (CPA) and/or after caffeine-induced release from the ryanodine-sensitive Ca^{2+} pool. As shown in *Figure 3D–G*, increases in $[Ca^{2+}]_i$ resulting from enhanced Ca^{2+} influx due to α_{1A}-AR stimulation with A61603 were observed after CPA pre-treatment, which depletes intracellular stores and

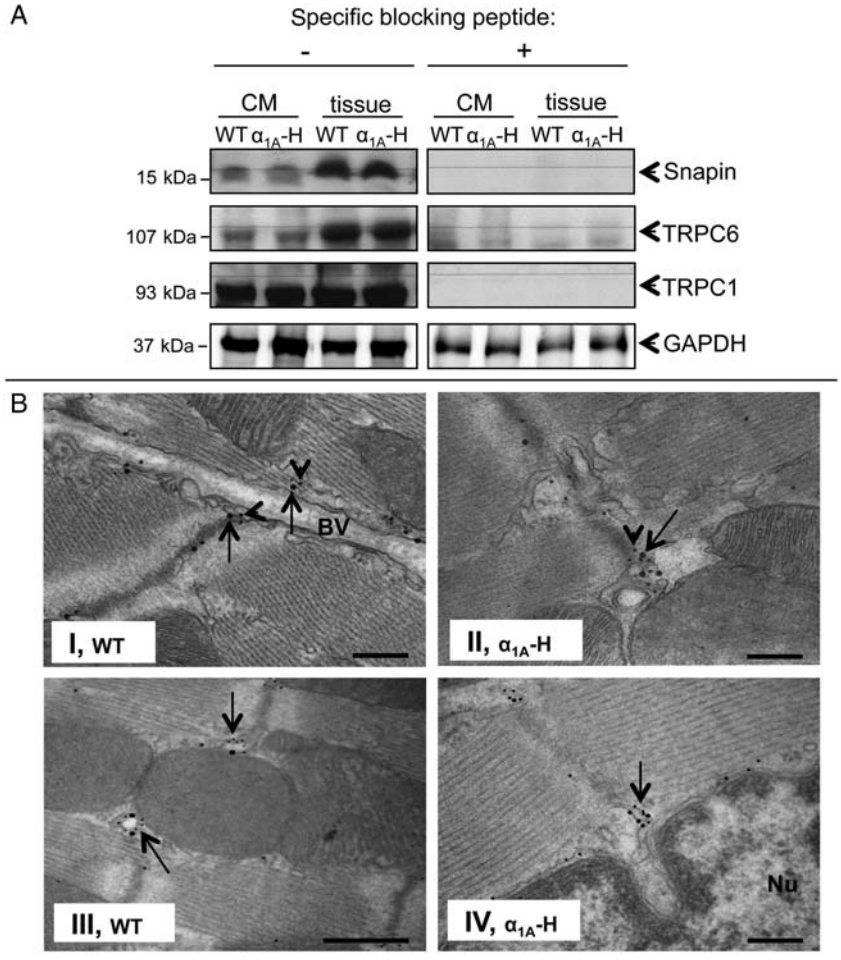

Figure 1 Snapin, TRPC6, and TRPC1 expression in isolated CMs and heart tissue and localization in heart sections from α_{1A}-H and WT mice. (*A*) Solubilized membranes (120 μg) from WT or α_{1A}-H CMs or heart tissue were fractionated on 6% SDS–PAGE for TRPC6 (~107 kDa) and TRPC1 (~93 kDa) or 15% SDS–PAGE for Snapin (~15 kDa) followed by immunoblotting with anti-Snapin, or anti-TRPC6, or anti-TRPC1 antibody in the absence (−) (left panels) or presence (+) (right panels) of their specific peptide immunogen. As loading controls, solubilized membranes were similarly evaluated with anti-GAPDH antibody. (*B*) Double immunogold labelling with anti-TRPC6 (small—10 nm gold particles, arrowhead) and anti-Snapin (large—20 nm gold particles, arrow) antibodies. I and II show co-localization of TRPC6 and Snapin along the plasma membrane (I), and at the ends of sarcomere Z-lines localized to t-tubules. T-tubule localization of TRPC6 was confirmed by double immunogold labelling of anti-TRPC6 (10 nm particles) and t-tubule-specific anti-caveolin-3 antibodies (20 nm particles) (III and IV). Both proteins co-localize at the t-tubules (arrows). TRPC1 showed a similar pattern of expression to TRPC6 (not shown). BV, blood vessel; Nu, nucleus. Scale bars: I, II, and IV = 200 nm; III = 500 nm. Images were obtained using a JEOL1400 TEM microscope at ×50 000.

pre-activates SOCs.[27,28] Of interest, similar responses were observed in studies of single-isolated CMs where cells were pre-treated with both CPA and caffeine (see Supplementary material online, *Figure S3A*). Moreover, in both studies of CM batches (*Figure 3D* and *E*) and single-isolated CMs (see Supplementary material online, *Figure S3A*), α_{1A}-AR-stimulated Ca^{2+} influx was observed only if Ca^{2+} was present in the extracellular medium. Influx was not evident in the absence of extracellular Ca^{2+} but could be restored by the addition of external Ca^{2+} to α_{1A}-H CMs (*Figure 3F* and *G*; see Supplementary material online, *Figure S3B*). This was most evident in single-isolated α_{1A}-H CMs where SOCE activation after store depletion only caused a minor $[Ca^{2+}]_i$ increase when compared with the large increase observed after A61603 administration. The latter was more transient if cells were bathed in 1.8 mM Ca^{2+} throughout, but was marked and sustained when A61603 was applied under Ca^{2+}-free conditions and then 1.8 mM Ca^{2+} reintroduced to the external medium (see Supplementary material online, *Figure S3A* and *B*). Note that the sharp Ca^{2+} peaks in these recordings correspond to the short global transients following caffeine application or represent spontaneous Ca^{2+} waves.

To further delineate whether the A61603-mediated increase in $[Ca^{2+}]_i$ was due to SOCE or ROCE, α_{1A}-ARs on single-isolated CMs were blocked with the α_{1A}-selective antagonist, KMD3213, after depletion of SR Ca^{2+} stores, but before the addition (~150 s later) of Ca^{2+} to the external medium (see Supplementary material online, *Figure S3C*). In this situation, no increase in cytoplasmic Ca^{2+} was observed (see Supplementary material online, *Figure S3C*), arguing against a mechanism involving activation of SOCE, which would be expected to result in an influx of Ca^{2+}, independent of α_{1A}-AR activity. This scenario largely excludes SOCE, which is

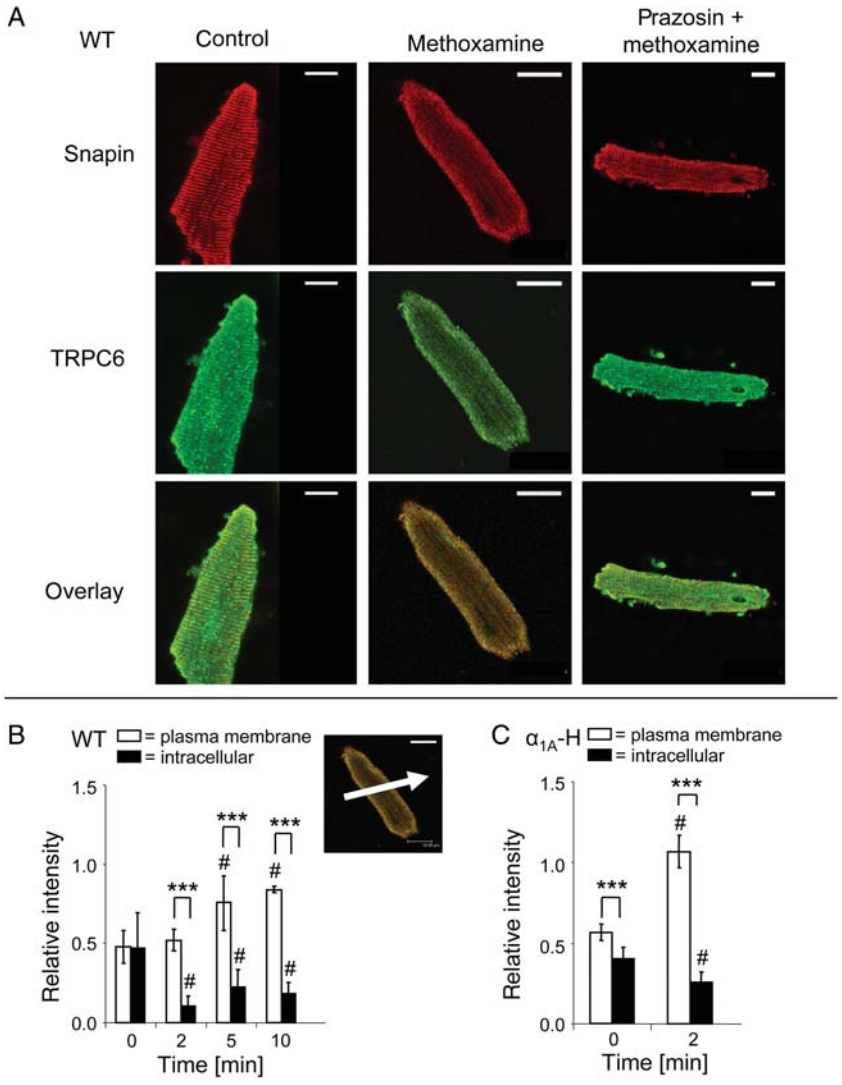

Figure 2 Subcellular distribution of TRPC6 and Snapin in CMs from WT and α_{1A}-H mice (*A*) before and after α_{1A}-AR activation with methoxamine (100 μM) in the absence or presence of prazosin (100 nM) [cells immunostained with anti-Snapin or anti-TRPC6 antibody and visualized by confocal microscopy; bottom row: overlay of TRPC6 and Snapin staining (yellow). Scale bar, 20 μm. α_{1A}-H CMs showed similar distribution of Snapin and TRPC6 (not shown)], and (*B* and *C*) quantitative morphometry of TRPC6 and Snapin subcellular distribution [overlay of Snapin and TRPC6 staining (see inset) in (*B*) WT and (*C*) α_{1A}-H CMs, before and after stimulation with methoxamine (100 μM). Relative intensity: intensity of staining relative to the mean pixel intensity after background subtraction. Bar graphs: averaged pixel intensity units (±1SD) from at least eight samples stained with anti-TRPC6 or anti-Snapin antibody for each time point, >10 trajectories across the cell (white arrow in the inset shows a representative trajectory). ***$P < 0.001$ for comparisons indicated, $^{\#}P < 0.001$ relative to respective basal]. $n = 3–4$ (in duplicate) for each condition.

known to be restricted to an α_{1A}-AR-activation-independent Stim1–Orai1 interaction.[29] To verify that α_{1A}-AR-mediated Ca^{2+} influx is dependent on TRPC6 activity, cells were pre-incubated with anti-TRPC6 antibody and then α_{1A}-ARs were activated after store depletion in Ca^{2+}-free medium (see Supplementary material online, *Figure S3D*). This resulted in a continued decline in fluo-4 signal, most likely due to further Ca^{2+} efflux as a result of continued activity of sodium–calcium exchangers and plasma membrane Ca^{2+}-ATPases. After stimulation of α_{1A}-AR with A61603 and restoration of external Ca^{2+}, cytoplasmic Ca^{2+} failed to increase. Taken together, these results indicate that in α_{1A}-H CMs the increased $[Ca^{2+}]_i$ observed with activation of the α_{1A}-AR is mediated by ROCE, with no or only minor involvement of SOCE.

Furthermore, this ROCE requires full functional availability of TRPC6. Blockade of TRPC6 with the anti-TRPC6 antibody dose-dependently inhibited $[Ca^{2+}]_i$ increase resulting from α_{1A}-AR activation in cells studied in batches (*Figure 4A*) and in single-isolated CMs using one effective antibody concentration (see Supplementary material online, *Figure S3D*). In contrast to the very pronounced effect of the anti-TRPC6 antibody, the anti-TRPC1 antibody had a much smaller effect on A61603-mediated increases in cytoplasmic Ca^{2+} in α_{1A}-H CMs (*Figure 4A*). Moreover, neither TRPC1 nor TRPC6 pre-immune serum affected α_{1A}-AR-mediated increases in $[Ca^{2+}]_i$ (see Supplementary material online, *Figure S4*). Snapin knockdown also attenuated α_{1A}-AR-mediated Ca^{2+} entry. This is shown in *Figure 4B*, where Snapin knockdown was achieved by infection of CMs

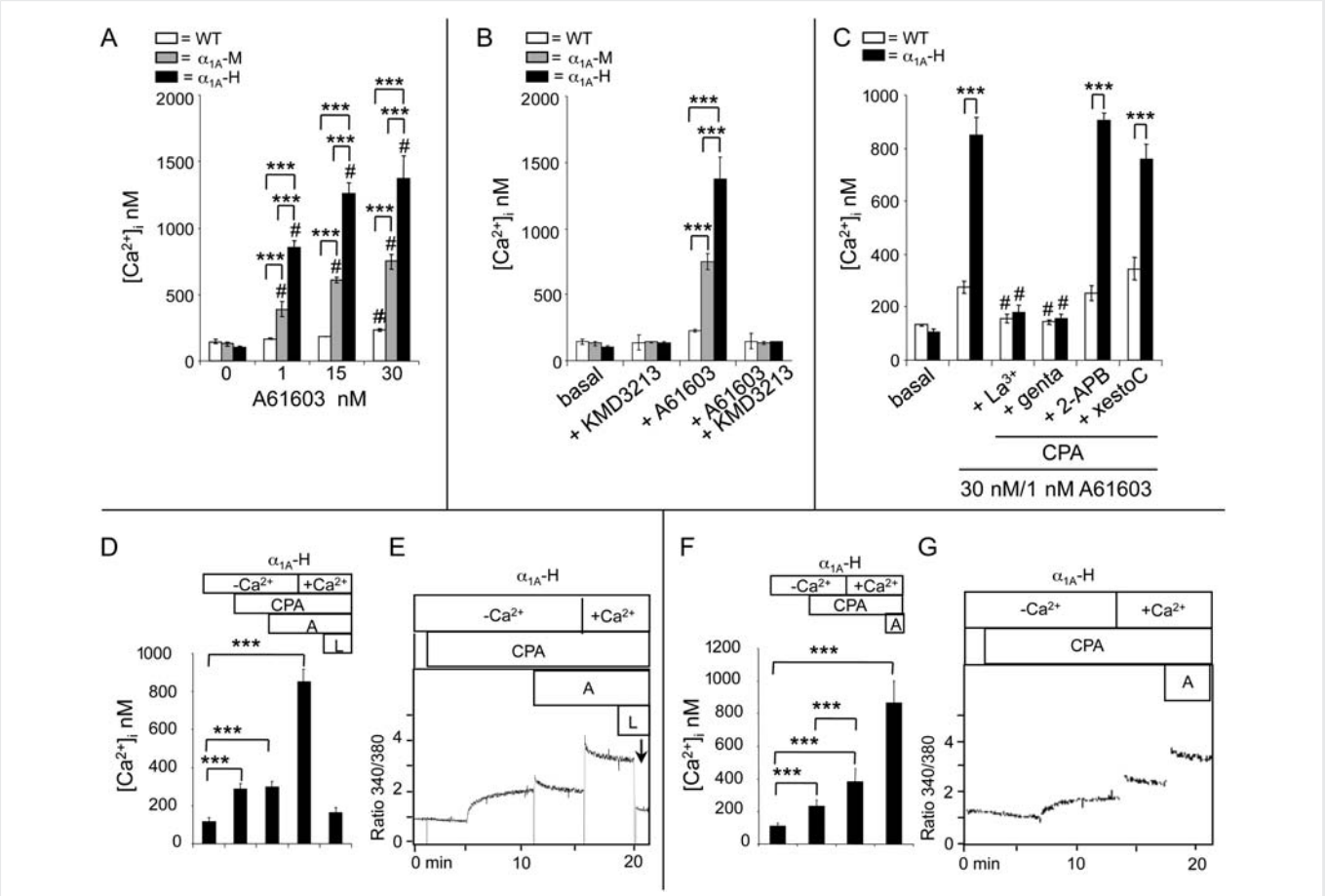

Figure 3 In response to α_{1A}-AR stimulation, isolated fura-2 AM-loaded CMs from α_{1A}-M and α_{1A}-H mice show a greater increase in $[Ca^{2+}]_i$ than those from WT CMs mediated by ROC- but not SOC-mediated Ca^{2+} entry. (*A*–*C*) $[Ca^{2+}]_i$ levels in batches of isolated CMs: (*A*) after treatment with the α_{1A}-agonist, A61603 (note: 30 nM A61603 in α_{1A}-H CMs caused cells to round, likely signifying cell death due to Ca^{2+} overload) or (*B*) after pre-treatment with α_{1A}-AR-antagonist, KMD3213 (500 nmol/L), prior to A61603 (30 nmol/L) ($^{\#}P < 0.001$ vs. respective basal values), or (*C*) after CPA (10 μmol/L) addition and then α_{1A}-AR activation with 30 nmol/L (WT) or 1 nmol/L (α_{1A}-H) A61603 ± pre-treatment with La^{3+} (1 μmol/L), gentamicin (200 μmol/L), 2-APB (50 μmol/L), or xestospongin C (20 μmol/L) ($^{\#}P < 0.001$ for response in the presence of inhibitors vs. A61603 alone). (*D*–*G*) $[Ca^{2+}]_i$ levels in CMs after CPA (10 μmol/L) addition in nominally Ca^{2+}-free buffer ($-Ca^{2+}$), followed by the addition of (*D*) A61603 (A, 1 nmol/L), then 1.8 mmol/L $CaCl_2$ ($+Ca^{2+}$), then La^{3+} (L, 1 μmol/L), or (*F*) 1.8 mmol/L $CaCl_2$ ($+Ca^{2+}$), then A61603 (A, 1 nmol/L). (*E* and *G*) Representative traces of $[Ca^{2+}]_i$ transients shown in (*D*) and (*F*). Bars show $[Ca^{2+}]_i$ levels both basally and during the tonic phase of Ca^{2+} entry at 4 min. $n = 2–3$ (in duplicate) for each condition.

with either of two adenoviruses encoding anti-Snapin shRNA. In contrast, α_{1A}-AR-mediated Ca^{2+} entry was evident in uninfected CMs or in cells infected with an adenovirus encoding a scrambled anti-Snapin shRNA. Functionality and specificity of anti-Snapin-specific shRNA-adenoviruses was demonstrated by reverse transcriptase–polymerase chain reaction and immunoblotting (see Supplementary material online, *Figure S5*), where the steady-state level of Snapin mRNA was markedly suppressed 96 h after adenoviral infection with either Snapin-specific shRNA adenovirus, as was Snapin protein expression. In contrast, in CMs infected with adenovirus encoding scrambled anti-Snapin shRNA, Snapin transcript, and protein expression were unaltered. Snapin residues targeted by the two anti-Snapin shRNAs (shRNA1-Snapin and shRNA2-Snapin) are indicated in Supplementary material online, *Figure S5E*. Taken together, these findings indicate that both Snapin and TRPC6 are required for α_{1A}-AR-stimulated Ca^{2+} entry.

3.5 Snapin specifically couples TRPC6 to the α_{1A}-AR

$G_{q/11}$-coupled angiotensin-II type 1 receptors (AT_1) are expressed in the heart and can activate TRPC6 in CMs.[30] As shown in *Figure 4C*, Angiotensin II (Ang II, 100 nM) stimulation of α_{1A}-H and WT CMs-induced equivalent increases in $[Ca^{2+}]_i$ that were markedly reduced by TRPC6 inhibition, but not by Snapin knockdown. This indicates that although α_{1A}-AR-mediated TRPC6 activation is Snapin-dependent, TRPC6 activation by another Gq-coupled G protein-coupled receptor (GPCR), that for Ang II, is not.

3.6 Essential role of PLCβ in α_{1A}-AR-stimulated Ca^{2+} entry

Inhibition of PLCβ by U-73122 (but not its inactive enantiomer, U73343) suppressed α_{1A}-AR-stimulated increases in $[Ca^{2+}]_i$ in both

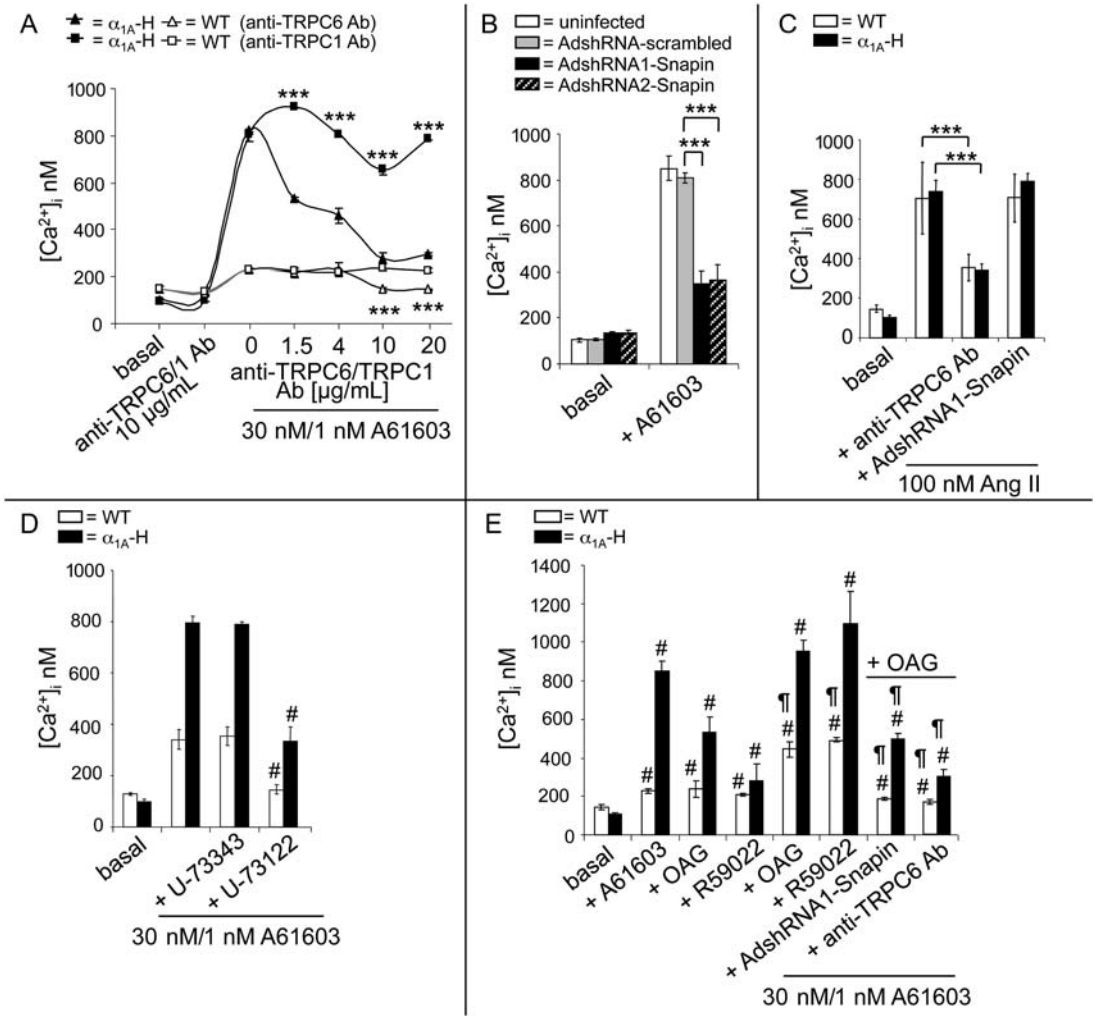

Figure 4 α_{1A}-AR-mediated Ca^{2+} entry in CMs requires Snapin, TRPC6, and the Gq-PLCβ-DAG pathway. (*A*) $[Ca^{2+}]_i$ levels in batches of fura-2 AM-loaded isolated CMs pre-incubated for 30 min with anti-TRPC1 or TRPC6 antibody (0, 1.5, 4, 10, or 20 μg/mL), and then activated with A61603 (30 nM WT; 1 nM α_{1A}-H). ***$P < 0.001$ for responses in the presence of anti-TRPC1 vs. anti-TRPC6. (*B–E*) $[Ca^{2+}]_i$ levels in batches of fura-2 AM-loaded isolated CMs: (*B*) treated with A61603 (1 nmol/L) in uninfected, or AdshRNA-scrambled- or AdshRNA1-Snapin or AdshRNA2-Snapin-infected (96 h in each case) α_{1A}-H CMs; (*C*) treatment with Ang II (100 nmol/L) ± 96 h pre-treatment with AdshRNA1-Snapin or pre-incubation with anti-TRPC6 antibody. ***$P < 0.001$ for comparisons indicated; ns, not significant; (*D*) treatment with A61603 (30 nmol/L WT; 1 nmol/L α_{1A}-H) ± pre-treatment with U-73343 (5 μmol/L), U-73122 (5 μmol/L), or Go6976 (1 μmol/L), $^{\#}P < 0.001$ relative to respective responses with A61603 alone; (*E*) treatment with A61603 (30 nmol/L WT; 1 nmol/L α_{1A}-H) or after pre-treatment with OAG (100 μmol/L) or R59022 (10 μmol/L) followed by ± A61603 treatment, or after 96 h pre-treatment with AdshRNA1-Snapin followed by OAG and then A61603, or after pre-incubation with anti-TRPC6 antibody (10 μg/mL) followed by OAG and A61603 ($^{\#}P < 0.001$ relative to respective basal values; $^{\P}P < 0.001$ relative to respective responses with A61603 alone). Bars show $[Ca^{2+}]_i$ levels both basally and during the tonic phase of Ca^{2+} entry at 4 min. $n = 2–3$ (in duplicate) for each condition.

α_{1A}-H and WT CMs (*Figure 4D*). Also, increasing DAG levels by the addition of the membrane permeable DAG analogue, 1-oleoyl-2-acetyl-sn-glycerol (OAG), or by the inhibition of DAG metabolism with R59022, a DAG lipase inhibitor, increased $[Ca^{2+}]_i$ and enhanced the increase in $[Ca^{2+}]_i$ observed with α_{1A}-AR activation alone in WT CMs (*Figure 4E*), which is likely due to direct activation of TRPC6 by DAG.[31] However, despite administration of OAG at the same concentration that alone increased $[Ca^{2+}]_i$, in α_{1A}-H and WT CMs, Snapin knockdown, or TRPC6 blockade suppressed A61603-stimulated increases in $[Ca^{2+}]_i$ in both α_{1A}-H and WT CMs (*Figure 4E*). These findings indicate that α_{1A}-AR/Snapin/TRPC6-mediated Ca^{2+} entry is augmented by PLCβ-mediated DAG production via an effect at the level of TRPC6.

3.7 Increases in cardiac contractility in WT and α_{1A}-AR-H mice and sudden cardiac death of α_{1A}-H mice is prevented by blockade of α_{1A}-ARs or TRPC6

We reported previously that α_{1A}-H mice die prematurely of sudden cardiac death manifested by a progressive reduction in QRS amplitude and then in left ventricular pressure.[20] To investigate whether this

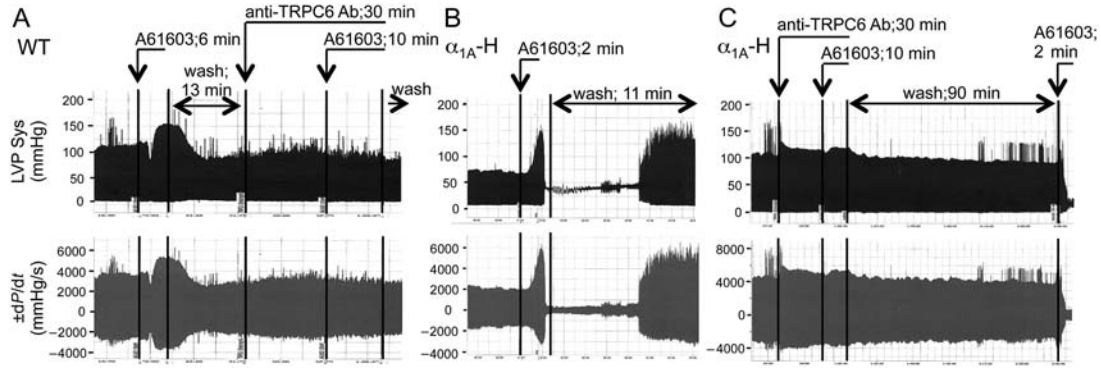

Figure 5 TRPC6-blockade prevents A61603-induced contractility in Langendorff-perfused WT hearts, and A61603-induced sudden cardiac death in isolated α_{1A}-H hearts. Representative LV systolic pressure (LVP Sys; mmHg/s) and $\pm dP/dt$ (mmHg/s) traces from (*A*) WT, or (*B*), (*C*), α_{1A}-H hearts, before and after A61603 (100 nmol/L) $\pm$anti-TRPC6 antibody (Ab; 10 μg/mL), administered at the times indicated (arrows). Data are representative of similar responses in seven to eight hearts.

response involved Ca^{2+} entry via α_{1A}-AR-stimulated TRPC6 activation, we used isolated perfused hearts from α_{1A}-H mice. As shown in *Figure 5B*, activation of α_{1A}-ARs with A61603 mimicked the sudden cardiac death response observed in intact animals, and A61603 washout restored heart function. Administration of either KMD3213 (data not shown) or anti-TRPC6 antibody, but not anti-TRPC1 antibody (data not shown), before A61603-stimulation, prevented the hypercontractile response in both α_{1A}-H and WT hearts, and completely protected α_{1A}-H hearts from sudden cardiac death (*Figure 5A* and *C*). The cardiac haemodynamics in WT and α_{1A}-H Langendorff-perfused hearts are given in Supplementary material online, *Table S1*. These findings provide evidence that α_{1A}-AR-mediated activation of TRPC6 is a physiologically relevant pathway underlying α_{1A}-AR-mediated cardiac contractile responses in WT mice and is pathophysiologically involved in sudden cardiac death of α_{1A}-H mice.

4. Discussion

Myocardial α_1-AR signalling pathways remain poorly defined, partly because of low levels of α_1-AR expression and, thus, limited signal output in normal heart under physiological conditions. The signalling pathway mediating positive inotropic effects of α_1-ARs has been studied for >30 years but remains enigmatic. The increase in $[Ca^{2+}]_i$ associated with α_1-AR activation in the normal heart is relatively small compared with the increase in force, suggesting that a receptor-stimulated increase in Ca^{2+} sensitivity is importantly involved in receptor-coupled increase in contractility.[32] However, in skinned fibre preparations, pCa^{2+}-force curves are unaltered between α_1-H and WT preparations (Z.-Y. Yu, J.-C. Tan, A.C. McMahon, S.E. Iismaa, X.-H. Xiao, S.H. Kesteven, M.E. Reichelt, M.C. Mohl, D. Fatkin, D.G. Allen, S.I. Head, R.M. Graham, M.P. Feneley, unpublished observations). Here, we took advantage of an α_{1A}-H transgenic mouse model with enhanced cardiac α_{1A}-AR expression and activity to investigate α_{1A}AR-coupled signalling. Based on our findings, we present a model for α_{1A}-AR-coupled cardiac Ca^{2+} entry involving redirection and activation of TRPC6 from the cytoplasm to the plasmalemma via interaction with Snapin. This in turn enhances cardiac contractility. TRPC6-mediated Ca^{2+} entry is also partially modulated by α_{1A}AR-stimulated activation of $G_{q/11}$, and, thus, PLCβ, which results in DAG production that independently activates TRPC6 in the plasma membrane (*Figure 6*). In support of this novel α_{1A}-AR-coupled signalling pathway, we show: (i) interaction of α_{1A}-AR-Snapin-TRPC6, which is increased *in vivo* in the absence of α_{1A}-agonist in α_{1A}-H relative to WT hearts, and is further enhanced by α_{1A}-AR activation; (ii) α_{1A}-AR-mediated translocation of TRPC6 and Snapin from the cytosol to the plasma membrane; (iii) dose-related increases in CM $[Ca^{2+}]_i$ proportional to the level of α_{1A}-AR expression and sensitive to α_{1A}-AR inhibition, TRPC6 blockade, or Snapin knockdown; (iv) increased α_{1A}-AR-stimulated CM $[Ca^{2+}]_i$ sensitive to inhibition of PLC and augmented by inhibition of DAG metabolism or by administration of the DAG analogue OAG and (v) α_{1A}-AR-mediated increases in $[Ca^{2+}]_i$ mediated by activation of ROCE rather than SOCE, since (a) inhibition of SOC activity or of IP_3Rs and SERCA did not block α_{1A}-AR-stimulated increases in $[Ca^{2+}]_i$, and (b) depletion of SR stores in the absence of extracellular Ca^{2+} inhibited α_{1A}-AR-mediated Ca^{2+} influx and was restored by the addition of Ca^{2+} only when the α_{1A}-AR–TRPC6 interaction was preserved; and (vi) most intriguingly, antibody-mediated blockade of TRPC6 not only inhibited α_{1A}-AR-mediated increases in cardiac contractility in WT and α_{1A}-H hearts, but also prevented α_{1A}-AR-stimulated Ca^{2+}-induced sudden cardiac death in α_{1A}-H mice. Studies in vascular smooth muscle and other non-cardiac tissues such as brain and neuronal cell lines support our finding that TRPC6 serves as an α_{1A}-AR-stimulated Ca^{2+}-permeable cation channel that mediates increased $[Ca^{2+}]_i$,[14,33] although in those studies, the adaptor function of Snapin was not evaluated. In our studies, α_{1A}-AR-stimulated TRPC6 activation is clearly DAG-sensitive and independent of IP_3-signalling. Although IP_3 is a documented regulator of $[Ca^{2+}]_i$ in non-cardiac cells, its role in CMs is questionable, since IP_3 production is not increased in α_{1A}-H mice.[17] Nonetheless, despite the low levels of IP_3R expression in CMs, IP_3R-mediated increases in nuclear $[Ca^{2+}]$ appear to underlie endothelin-1 (ET-1)-stimulated hypertrophy.[34]

Like α_{1A}-ARs, AT_1-receptors also couple to $G_{q/11}$ and have been reported to stimulate Ca^{2+} entry via TRPC6 activation.[30] However, AT_1-receptor coupling to TRPC6 does not involve Snapin. Instead, Snapin appears to be an α_{1A}-AR-specific adaptor protein that does

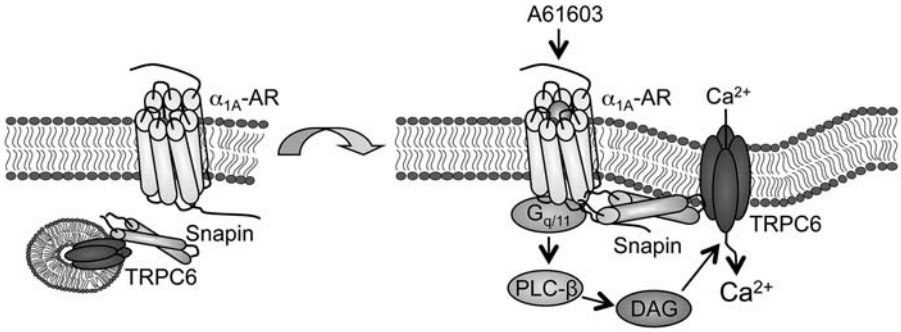

Figure 6 Schematic of α_{1A}-AR signalling pathway mediating cardiac contractility in WT CMs and sudden cardiac death in α_{1A}-H CMs. This involves α_{1A}-AR/Snapin/TRPC6 ternary complex formation and translocation to the plasma membrane, resulting in sustained Ca^{2+} entry. α_{1A}-AR-mediated activation of TRPC6 is also dependent on DAG production via PLC activation.

not interact promiscuously with other $G_{q/11}$PCRs since (i) Snapin knockdown failed to inhibit Ang-II-stimulated increases in $[Ca^{2+}]_i$, and (ii) a BLAST search of the α_{1A}-AR sequence that specifically interacts with Snapin[12] shows no homology with any other GPCR.

Our data show that in CMs, TRPC6 and Snapin co-localize along the plasma membrane and at the end of sarcomere Z-lines, even in the absence of α_{1A}-AR stimulation, suggesting that they interact in a pre-formed complex to facilitate rapid ROCE. Consistent with preferential sarcolemmal localization of TRPC6 observed in CMs from cardiac-specific TRPC6 overexpressing mice,[35] we found translocation of Snapin and TRPC6 to the plasma membrane following α_{1A}-AR stimulation. We do not yet know whether α_{1A}-AR stimulation also results in Snapin and TRPC6 translocation to the t-tubules—structures that house important signalling molecules, such as L-type Ca^{2+} channels that are involved in β-AR-mediated excitation–contraction coupling.

Recent findings indicate a role of TRPC channels and TRPC6 in hypertrophy[12] but not contraction. Differential localization may have important functional consequences that may underlie the enhanced cardiac contractility mediated by α_{1A}-AR-stimulated Ca^{2+} entry via TRPC6, and the lack of hypertrophy in α_{1A}-H mice. By analogy, excitation–contraction-induced increases in $[Ca^{2+}]_i$ in CMs are restricted to the cytosol, whereas the increase in $[Ca^{2+}]_i$ due to ET-1 stimulation is restricted to the nucleus.[34] Thus, Ca^{2+} entry via α_{1A}-AR-stimulated TRPC6 channels may be restricted to juxta-membranous microdomains at sites distinct from those involved in β-AR-stimulated Ca^{2+} entry.[36]

In addition to physiologically regulating α_{1A}-AR-stimulated cardiac contractility in WT mice, TRPC6, at least to some extent, also appears to be critically involved in the pathophysiology of the sudden cardiac death observed in α_{1A}-H mice observed in response to increased sympathetic activity. Prevention of sudden cardiac death by α_{1A}-AR blockade and independently by TRPC6 blockade indicates that this response is a result of excessive α_{1A}-AR-mediated Ca^{2+} entry via TRPC6. Excessive Ca^{2+} is known to inhibit gap junction conductance[37]—an effect entirely consistent with the progressive reduction in QRS amplitude without arrhythmias in α_{1A}-H mice, but one that contrasts with the ventricular fibrillation and sudden cardiac death observed with store-overload-induced Ca^{2+} release.[38]

In vivo, the α_{1A}-H model displays a robust increase in systolic contractility (dP/dt_{max}) with little change in diastolic relaxation (dP/dt_{min}) and no hypertrophy.[17] Thus, receptor-coupled signalling pathways for contractility and hypertrophy may be spatially and temporally dissociated in CMs, despite the seeming commonality of enhanced $[Ca^{2+}]_i$ being required for both. In agreement with this notion is the finding that under physiological conditions, activation of gene transcription programmes can be dissociated from enhanced $[Ca^{2+}]_i$ following activation of the prototypical pro-proliferative receptor, the epidermal growth factor receptor.[39]

In summary, we have delineated a novel myocardial α_{1A}-AR signalling pathway that provides significant insights into receptor-regulated cardiac contractility and Ca^{2+} handling in the context of both WT α_{1A}-AR expression, and receptor overexpression. Given that the transgenic model of enhanced α_{1A}-AR activity displays robust hypercontractility but no hypertrophy, our data suggest that modest activation of the α_{1A}-AR-Snapin-TRPC6-pathway may be a promising approach for therapeutically augmenting cardiac performance in clinical settings of impaired cardiac performance, such as myocardial infarction or heart failure.

Supplementary material

Supplementary material is available at *Cardiovascular Research* online.

Acknowledgements

We thank Susanne Lutz, Department of Pharmacology, University Hospital, Goettingen for the pAdTrack-si Vector and Elizabeth A. Woodcock for useful advice and critical review of the work.

Conflict of interest: none declared.

Funding

This work was supported by the National Health and Medical Research Council (grant numbers 573732 to R.M.G., 526622 to S.E.I.), National Heart Foundation of Australia (grant number 635521 to R.M.G.), and the German Academic Exchange Service (DAAD; grant number 50321104 to O.F.).

References

1. Woodcock EA, Du XJ, Reichelt ME, Graham RM. Cardiac alpha 1-adrenergic drive in pathological remodelling. *Cardiovasc Res* 2008;**77**:452–462.
2. Skomedal T, Schiander IG, Osnes JB. Both alpha and beta adrenoceptor-mediated components contribute to final inotropic response to norepinephrine in rat heart. *J Pharmacol Exp Ther* 1988;**247**:1204–1210.

3. Sjaastad I, Schiander I, Sjetnan A, Qvigstad E, Bokenes J, Sandnes D *et al*. Increased contribution of alpha 1- vs. beta-adrenoceptor-mediated inotropic response in rats with congestive heart failure. *Acta Physiol Scand* 2003;**177**:449–458.
4. Petrashevskaya NN, Bodi I, Koch SE, Akhter SA, Schwartz A. Effects of alpha1-adrenergic stimulation on normal and hypertrophied mouse hearts. Relation to caveolin-3 expression. *Cardiovasc Res* 2004;**63**:561–572.
5. Milano CA, Dolber PC, Rockman HA, Bond RA, Venable ME, Allen LF *et al*. Myocardial expression of a constitutively active alpha 1B-adrenergic receptor in transgenic mice induces cardiac hypertrophy. *Proc Natl Acad Sci USA* 1994;**91**:10109–10113.
6. O'Connell TD, Swigart PM, Rodrigo MC, Ishizaka S, Joho S, Turnbull L *et al*. Alpha1-adrenergic receptors prevent a maladaptive cardiac response to pressure overload. *J Clin Invest* 2006;**116**:1005–1015.
7. Mizuno N, Itoh H. Functions and regulatory mechanisms of Gq-signaling pathways. *Neurosignals* 2009;**17**:42–54.
8. Roberts-Thomson SJ, Peters AA, Grice DM, Monteith GR. ORAI-mediated calcium entry: mechanism and roles, diseases and pharmacology. *Pharmacol Ther* 9999;**127**:121–130.
9. Berridge MJ, Bootman MD, Lipp P. Calcium—a life and death signal. *Nature* 1998;**395**:645–648.
10. Marks AR. Cardiac intracellular calcium release channels: role in heart failure. *Circ Res* 2000;**87**:8–11.
11. Abramowitz J, Birnbaumer L. Physiology and pathophysiology of canonical transient receptor potential channels. *Faseb J* 2009;**23**:297–328.
12. Eder P, Molkentin JD. TRPC channels as effectors of cardiac hypertrophy. *Circ Res* 2011;**108**:265–272.
13. Plant TD, Schaefer M. Receptor-operated cation channels formed by TRPC4 and TRPC5. *Naunyn Schmiedebergs Arch Pharmacol* 2005;**371**:266–276.
14. Suzuki F, Morishima S, Tanaka T, Muramatsu I. Snapin, a new regulator of receptor signaling, augments alpha1A-adrenoceptor-operated calcium influx through TRPC6. *J Biol Chem* 2007;**282**:29563–29573.
15. Ilardi JM, Mochida S, Sheng ZH. Snapin: a SNARE-associated protein implicated in synaptic transmission. *Nat Neurosci* 1999;**2**:119–124.
16. Gromley A, Yeaman C, Rosa J, Redick S, Chen CT, Mirabelle S *et al*. Centriolin anchoring of exocyst and SNARE complexes at the midbody is required for secretory-vesicle-mediated abscission. *Cell* 2005;**123**:75–87.
17. Lin F, Owens WA, Chen S, Stevens ME, Kesteven S, Arthur JF *et al*. Targeted alpha(1A)-adrenergic receptor overexpression induces enhanced cardiac contractility but not hypertrophy. *Circ Res* 2001;**89**:343–350.
18. Du XJ, Fang L, Gao XM, Kiriazis H, Feng X, Hotchkin E *et al*. Genetic enhancement of ventricular contractility protects against pressure-overload-induced cardiac dysfunction. *J Mol Cell Cardiol* 2004;**37**:979–987.
19. Du XJ, Gao XM, Kiriazis H, Moore XL, Ming Z, Su Y *et al*. Transgenic alpha1A-adrenergic activation limits post-infarct ventricular remodeling and dysfunction and improves survival. *Cardiovasc Res* 2006;**71**:735–743.
20. Chaulet H, Lin F, Guo J, Owens WA, Michalicek J, Kesteven SH *et al*. Sustained augmentation of cardiac alpha1A-adrenergic drive results in pathological remodeling with contractile dysfunction, progressive fibrosis and reactivation of matricellular protein genes. *J Mol Cell Cardiol* 2006;**40**:540–552.
21. Cuello F, Bardswell SC, Haworth RS, Yin X, Lutz S, Wieland T *et al*. Protein kinase D selectively targets cardiac troponin I and regulates myofilament Ca2+ sensitivity in ventricular myocytes. *Circ Res* 2007;**100**:864–873.
22. He TC, Zhou S, da Costa LT, Yu J, Kinzler KW, Vogelstein B. A simplified system for generating recombinant adenoviruses. *Proc Natl Acad Sci USA* 1998;**95**:2509–2514.
23. Terracciano CM, MacLeod KT. Measurements of Ca2+ entry and sarcoplasmic reticulum Ca2+ content during the cardiac cycle in guinea pig and rat ventricular myocytes. *Biophys J* 1997;**72**:1319–1326.
24. Zhou YY, Wang SQ, Zhu WZ, Chruscinski A, Kobilka BK, Ziman B *et al*. Culture and adenoviral infection of adult mouse cardiac myocytes: methods for cellular genetic physiology. *Am J Physiol Heart Circ Physiol* 2000;**279**:H429–H436.
25. Williams IA, Allen DG. Intracellular calcium handling in ventricular myocytes from mdx mice. *Am J Physiol Heart Circ Physiol* 2007;**292**:H846–H855.
26. Spassova MA, Soboloff J, He LP, Hewavitharana T, Xu W, Venkatachalam K *et al*. Calcium entry mediated by SOCs and TRP channels: variations and enigma. *Biochim Biophys Acta* 2004;**1742**:9–20.
27. Seidler NW, Jona I, Vegh M, Martonosi A. Cyclopiazonic acid is a specific inhibitor of the Ca2+-ATPase of sarcoplasmic reticulum. *J Biol Chem* 1989;**264**:17816–17823.
28. Pessah IN, Stambuk RA, Casida JE. Ca2+-activated ryanodine binding: mechanisms of sensitivity and intensity modulation by Mg2+, caffeine, and adenine nucleotides. *Mol Pharmacol* 1987;**31**:232–238.
29. Volkers M, Rohde D, Goodman C, Most P. S100A1: a regulator of striated muscle sarcoplasmic reticulum Ca2+ handling, sarcomeric, and mitochondrial function. *J Biomed Biotechnol* 2010;**2010**:178614.
30. Onohara N, Nishida M, Inoue R, Kobayashi H, Sumimoto H, Sato Y *et al*. TRPC3 and TRPC6 are essential for angiotensin II-induced cardiac hypertrophy. *EMBO J* 2006;**25**:5305–5316.
31. Gudermann T, Hofmann T, Mederos y Schnitzler M, Dietrich A. Activation, subunit composition and physiological relevance of DAG-sensitive TRPC proteins. *Novartis Found Symp* 2004;**258**:103–118; discussion 118–122, 155–109, 263–106.
32. Grimm M, Haas P, Willipinski-Stapelfeldt B, Zimmermann WH, Rau T, Pantel K *et al*. Key role of myosin light chain (MLC) kinase-mediated MLC2a phosphorylation in the alpha 1-adrenergic positive inotropic effect in human atrium. *Cardiovasc Res* 2005;**65**:211–220.
33. Inoue R, Okada T, Onoue H, Hara Y, Shimizu S, Naitoh S *et al*. The transient receptor potential protein homologue TRP6 is the essential component of vascular alpha(1)-adrenoceptor-activated Ca(2+)-permeable cation channel. *Circ Res* 2001;**88**:325–332.
34. Higazi DR, Fearnley CJ, Drawnel FM, Talasila A, Corps EM, Ritter O *et al*. Endothelin-1-stimulated InsP3-induced Ca2+ release is a nexus for hypertrophic signaling in cardiac myocytes. *Mol Cell* 2009;**33**:472–482.
35. Kuwahara K, Wang Y, McAnally J, Richardson JA, Bassel-Duby R, Hill JA *et al*. TRPC6 fulfills a calcineurin signaling circuit during pathologic cardiac remodeling. *J Clin Invest* 2006;**116**:3114–3126.
36. Bruton JD, Katz A, Westerblad H. Insulin increases near-membrane but not global Ca2+ in isolated skeletal muscle. *Proc Natl Acad Sci USA* 1999;**96**:3281–3286.
37. Firek L, Weingart R. Modification of gap junction conductance by divalent cations and protons in neonatal rat heart cells. *J Mol Cell Cardiol* 1995;**27**:1633–1643.
38. Jiang D, Chen W, Wang R, Zhang L, Chen SR. Loss of luminal Ca2+ activation in the cardiac ryanodine receptor is associated with ventricular fibrillation and sudden death. *Proc Natl Acad Sci USA* 2007;**104**:18309–18314.
39. Sawano A, Takayama S, Matsuda M, Miyawaki A. Lateral propagation of EGF signaling after local stimulation is dependent on receptor density. *Dev Cell* 2002;**3**:245–257.